NASA TECHNICAL NOTE

NASA TN D-5845

C. 1

NASA TN D-5845

TECH LIBRARY KAFB, NM

0132584

KIRTLAND AFB

HEAD TO BASE TRANSFER FUNCTION CHARACTERISTICS OF A CYLINDRICAL TANK PARTLY FILLED WITH LIQUID

by Carl F. Lorenzo, William G. Costakis, and Eva T. Jun

Lewis Research Center

Cleveland, Ohio 44135

NATIONAL AERONAUTICS AND SPACE ADMINISTRATION • WASHINGTON, D. C. • JUNE 1970

TECH LIBRARY KAFB, NM

0132584

1. Report No. NASA TN D-5845	2. Government Accession No.	3. Recipient's Catalog No.
4. Title and Subtitle HEAD TO BASE TRANSFER FUNCTION CHARACTERISTICS OF A CYLINDRICAL TANK PARTLY FILLED WITH LIQUID		5. Report Date June 1970
		6. Performing Organization Code
7. Author(s) Carl F. Lorenzo, William G. Costakis, and Eva T. Jun		8. Performing Organization Report No. E-5288
9. Performing Organization Name and Address Lewis Research Center National Aeronautics and Space Administration Cleveland, Ohio 44135		10. Work Unit No. 124-09
		11. Contract or Grant No.
12. Sponsoring Agency Name and Address National Aeronautics and Space Administration Washington, D.C. 20546		13. Type of Report and Period Covered Technical Note
		14. Sponsoring Agency Code

15. Supplementary Notes

16. Abstract

This study presents an analysis of the transfer function of head motion to base motion for a thin-walled cylindrical tank partially filled with a liquid. This transfer function is part of the overall structural description for the analysis of POGO type instabilities in rocket vehicles. The analysis utilized the double Laplace transform to achieve a closed form approximate solution. An experimental verification of the analysis was performed using a cylindrical plastic tank containing water. The results clearly demonstrated the importance of considering fluid resonance effects on head to base reponse. Indeed, for at least two fluid heights the fluid mode effects dominated the mechanical modes for this transfer function.

17. Key Words (*Suggested by Author(s)*) Transfer function; Pogo; Structure dynamics; Propellant tank; Rocket vehicle	18. Distribution Statement Unclassified - unlimited

19. Security Classif. (of this report)	20. Security Classif. (of this page)	21. No. of Pages	22. Price*
Unclassified	Unclassified	40	$3.00

*For sale by the Clearinghouse for Federal Scientific and Technical Information
Springfield, Virginia 22151

HEAD TO BASE TRANSFER FUNCTION CHARACTERISTICS OF A CYLINDRICAL TANK PARTLY FILLED WITH LIQUID

by Carl F. Lorenzo, William G. Costakis, and Eva T. Jun

Lewis Research Center

SUMMARY

This study presents an analysis of the transfer function of head motion to base motion for a thin-walled cylindrical tank partially filled with a liquid. This transfer function is part of the overall structural description for the analysis of POGO type instabilities in rocket vehicles.

The analysis utilized the double Laplace transform to achieve a closed form approximate solution. An experimental verification of the analysis was performed using a cylindrical plastic tank containing water.

The results clearly demonstrated the importance of considering fluid resonance effects on head to base response. Indeed, for at least two fluid heights, the fluid mode effects dominated the mechanical modes for this transfer function.

INTRODUCTION

The dynamic instability of launch vehicles due to coupling of the vehicle structure (in the longitudinal mode) and the vehicle propulsion system continues to be a problem. Prediction and solution of this instability known as POGO requires dynamic descriptions of the vehicle structure, tankage, feed system, and engine and their intercouplings.

Significant analyses have been made into the overall stability problem (refs. 1 to 4). These studies generally assume that vehicle structural modes are available from a complete structural analysis or from vibration testing. A number of related studies dealing with the fluid-tank dynamic characteristics may be found in references 5 to 7. In particular, references 5 and 6 consider the tank structure and fluid combination as an equivalent single lump mode. Also the transfer function characteristics of the distributed fluid alone have been considered (ref. 7).

The fundamental structural description required for POGO analysis is the transfer function of tank base pressure (feedline inlet pressure) to engine gimble plane motion (fig. 1). For the vehicle upper tank this requires upper tank base motion as an input, from which tank base pressure can be determined. This in turn requires the transfer function from lower tank head motion to gimble plane motion, that is, head to base response for a cylindrical tank. Consideration of this type response has been made for a cylindrical shell connecting two masses (without fluid) (ref. 8). Also the excellent study of Kana and Chu (ref. 9) has numerically determined the head response with contained fluid.

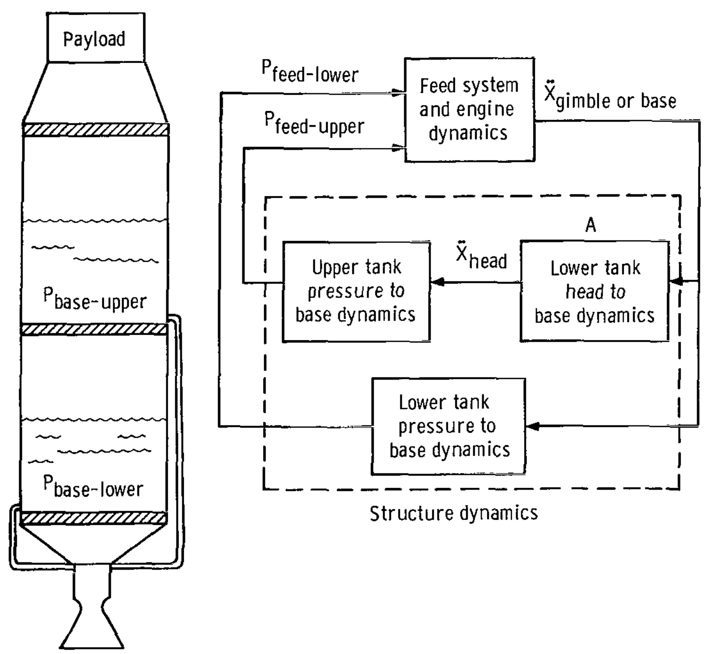

(a) Idealized vehicle.

(b) Block diagram.

Figure 1. - Simplified block diagram of idealized vehicle.

When the overall problem is considered in its simplest terms, the block diagram for POGO analysis of an idealized vehicle is shown in figure 1. In most current models block A is considered to be a single mode approximation to tank behavior - that is, a single mass (representing the fluid) together with appropriate springs coupling it to the remaining structure. However, it is clear that during a resonance of the fluid in the lower tank, lateral motion of the lower tank walls will influence the upper tank base motion and hence, the upper tank base pressure. This type of relation is also required to properly couple the upper tank to the payload.

This study presents a closed form approximation for the head to base response for a rigid base cylindrical tank partially filled with fluid. This analysis considers the distributed effects and the fluid pressure influences on shell motion. The model is not intended for detailed stability analysis, but as a tool in the early stages of vehicle design or for use in a rough cut at stability analysis.

An experiment was performed to support the analysis. A cylindrical plastic tank containing water was longitudinally excited. Resulting data were compared with the analytical model.

TRANSFER FUNCTION ANALYSIS

The following basic assumptions are made in the analysis of the shell-fluid system to obtain the desired response function:

(1) Shell and fluid are treated as one-dimensional in the longitudinal direction, and shell is distributed but has radial symmetry; that is, breathing and torsional modes are not considered.

(2) Shell bending and lateral dynamic effects are neglected; that is, laterally, the shell is a membrane.

(3) Fluid pressure response is assumed to depend only on tank base motion and is independent of wall motion except through acoustic velocity.

(4) Ullage gas pressure is assumed to be constant.

(5) Tank base and head are assumed rigid.

The coordinate system for the shell-fluid system is shown in figure 2. (Symbols are defined in appendix A.) The longitudinal displacement u of the shell is given by

$$\frac{\partial^2 u}{\partial x^2} - K_1 \frac{\partial u}{\partial t} - \frac{m_s}{D} \frac{\partial^2 u}{\partial t^2} = \frac{\nu}{R} \frac{\partial w}{\partial x} \tag{1}$$

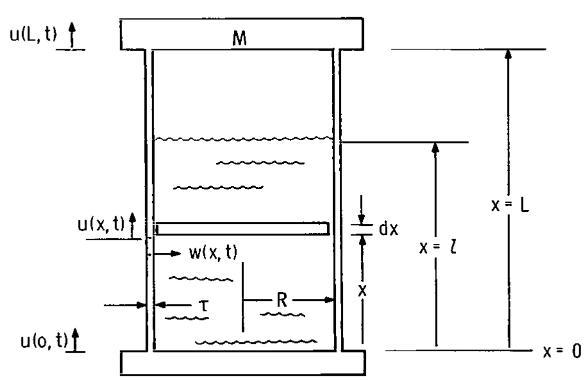

Figure 2. - Coordinate system.

(See, for example, refs. 10 and 11 with damping terms added.) The right side of this equation is a distributed forcing function which arises from the lateral motion of the wall. Also the $K_1(\partial u/\partial t)$ term is a distributed mechanical damping. The term $(\nu/R)(\partial w/\partial x)$ arises from the fluid pressures normal to the tank wall. These fluid pressures are determined using the equation (ref. 6, eq. (12))

$$\frac{\partial^2 p}{\partial x^2} = c^2 \frac{\partial^2 p}{\partial t^2} + K^* \frac{\partial p}{\partial t} \tag{2}$$

where

$$c^2 = \frac{\rho}{g}\left(B + \frac{2R}{E\tau}\right)$$

and

$$K^* = \frac{K}{A}\left(B + \frac{2R}{E\tau}\right)$$

The Laplace transform of equation (1) with respect to time t with all initial conditions zero is

$$\frac{\partial^2 U}{\partial x^2} - \left(K_1 s + \frac{m_s}{D} s^2\right)U = \frac{\nu}{R}\frac{\partial W}{\partial x} \tag{3}$$

in terms of the Laplace variable s. The solution of equation (2) for fluid pressure to base velocity for the boundary condition ($p(l, t)$ = Constant) is (ref. 7, eq. (38))

$$\frac{P(x, s)}{V(o, s)} = \frac{\rho}{g} \frac{s}{\sqrt{c^2 s^2 + K^* s}} \frac{\sinh\left[\sqrt{c^2 s^2 + K^* s}\,(l - x)\right]}{\cosh\left(\sqrt{c^2 s^2 + K^* s}\; l\right)} \qquad o \leq x \leq l \tag{4}$$

Now for the constant ullage pressure assumption, perturbations in fluid pressure do not influence longitudinal stress. Also when considering the shell as a membrane and neglecting lateral dynamics, the radial deflection is given by

$$W(x, s) = -\frac{R^2}{E\tau} P(x, s) = -\left(\frac{R^2\rho}{gE\tau}\right)\frac{sV(0, s)}{\sqrt{c^2s^2 + K^*s}} \frac{\sinh\left[\sqrt{c^2s^2 + K^*s}\ (l - x)\right]}{\cosh\left(\sqrt{c^2s^2 + K^*s}\ l\right)} \qquad o \leq x \leq l \tag{5}$$

Hence,

$$\frac{\nu}{R}\frac{\partial W(x, s)}{\partial x} = \left\{\begin{array}{ll} \frac{\nu R\rho}{gE\tau} sV(0, s)\left\{\frac{\cosh\left[\sqrt{c^2s^2 + K^*s}\ (l - x)\right]}{\cosh\left(\sqrt{c^2s^2 + K^*s}\ l\right)}\right\} & o \leq x \leq l \\ 0 \qquad l < x \leq L & \end{array}\right\} \tag{6}$$

This can also be expressed as

$$H(x, s) = \frac{\nu}{R}\frac{\partial W(x, s)}{\partial x} = \frac{\nu R\rho}{E\tau g}\frac{sV(o, s)\cosh\left[\sqrt{c^2s^2 + K^*s}\ (l - x)\right]}{\cosh\left(\sqrt{c^2s^2 + K^*s}\ l\right)}\left[1 - \mathcal{S}(x - l)\right] \tag{7}$$

where $\mathcal{S}(x - l)$ is a unit step function.

Since s is a parameter, equation (3) can be written as

$$\frac{d^2U}{dx^2} - \left(K_1 s + \frac{m_s}{D} s^2\right)U = H(x, s) \tag{8}$$

Applying the Laplace transform with respect to x, $\mathcal{L}_x$ (where p is the respective Laplace variable) yields

$$p^2\mathcal{U}(p, s) - pU(0^+, s) - \frac{dU}{dx}(0^+, s) - \left(K_1 s + \frac{m_s}{D} s^2\right)\mathcal{U}(p, s) = \mathcal{H}(p, s) \tag{9}$$

and letting $dU(0^+, s)/dx = q(s)$ gives equation (9) as

$$\mathcal{U}(p, s) = \frac{\mathcal{H}(p, s) + pU(0, s) + q(s)}{p^2 - \left(K_1 s + \frac{m_s}{D} s^2\right)} \tag{10}$$

The inverse Laplace transform with respect to p of equation (10) is (details of calculations shown in appendix B)

$$
U(x, s) = \begin{cases} \dfrac{\gamma}{2\alpha_2}\left\{\dfrac{\cosh(\alpha_2 x + \alpha_1 l)}{\alpha_1 + \alpha_2} - \dfrac{\cosh\left[\alpha_1(l - x)\right]}{\alpha_1 + \alpha_2} + \dfrac{\cosh\left[\alpha_1(x - l)\right]}{\alpha_1 - \alpha_2} - \dfrac{\cosh(\alpha_2 x - \alpha_1 l)}{\alpha_1 - \alpha_2}\right\} \\ \qquad + U(o, s)\cosh(\alpha_2 x) + \dfrac{q(s)}{\alpha_2}\sinh(\alpha_2 x) \qquad \text{for } 0 \le x \le l \\ \dfrac{\gamma}{2\alpha_2}\left\{\dfrac{\cosh(\alpha_2 x + \alpha_1 l)}{\alpha_1 + \alpha_2} - \dfrac{\cosh\left[\alpha_2(x - l)\right]}{\alpha_1 + \alpha_2} + \dfrac{\cosh\left[\alpha_2(x - l)\right]}{\alpha_1 - \alpha_2} - \dfrac{\cosh(\alpha_2 x - \alpha_1 l)}{\alpha_1 - \alpha_2}\right\} \\ \qquad + U(o, s)\cosh(\alpha_2 x) + \dfrac{q(s)}{\alpha_2}\sinh(\alpha_2 x) \qquad \text{for } l < x \le l \end{cases} \tag{11}
$$

where

$$
\alpha_1 = \sqrt{c^2 s^2 + K^* s}
$$

$$
\alpha_2 = \sqrt{\frac{m_s}{D}\, s^2 + K_1 s}
$$

$$
\gamma = \frac{\nu R \rho}{E \tau g}\, \frac{sV(o, s)}{\cosh(\alpha_1 l)}
$$

At the tank top ($x = L > l$)

$$
U(L, s) = \frac{\gamma}{2\alpha_2}\left\{\frac{\cosh(\alpha_2 L + \alpha_1 l)}{\alpha_1 + \alpha_2} + \frac{2\alpha_2 \cosh\left[\alpha_2(L - l)\right]}{\alpha_1^2 - \alpha_2^2} - \frac{\cosh(\alpha_2 L - \alpha_1 l)}{\alpha_1 - \alpha_2}\right\}
$$

$$
+ U(o, s)\cosh(\alpha_2 L) + \frac{q(s)}{\alpha_2}\sinh(\alpha_2 L) \qquad \text{for} \quad x = L \tag{12}
$$

The function $q(s)$ required for these equations is determined by consideration of the head boundary conditions.

Head Boundary Condition

The head and mechanical components above it are considered in terms of a mechanical impedance Z_m; hence,

$$Z_m = \frac{F}{V} = \frac{F}{sU(L,s)} \tag{13}$$

Then from the boundary condition at the top of the tank (ref. 7, for example)

$$F = sZ_m U(L,s) = -\frac{2\pi R\tau E}{1-\nu^2}\left(\frac{dU}{dx} - \frac{\nu W}{R}\right)\Bigg|_{x=L} \tag{14}$$

Since the radial deflection at $x = L$ is zero and after rearranging

$$\frac{dU}{dx}\Bigg|_{x=L} = C_1(s)U(L,s) \tag{15}$$

where

$$C_1(s) = -\left[\frac{sZ_m(1-\nu^2)}{2\pi R\tau E}\right] \tag{16}$$

Now, evaluating $dU/dx(L,s)$ and $U(L,s)$ from equations (11) and (12), respectively, substituting into equation (15), and solving for $q(S)/U(o,s)$ yield

$$\frac{q(s)}{U(o,s)} = \frac{1}{\frac{C_1}{\alpha_2}\sinh(\alpha_2 L) - \cosh(\alpha_2 L)}\left(\frac{\beta s^2}{2}\left\{\frac{\sinh(\alpha_2 L + \alpha_1 l)}{\alpha_1 + \alpha_2} + \frac{2\alpha_2 \sinh\left[\alpha_2(L - l)\right]}{\alpha_1^2 - \alpha_2^2}\right.\right.$$

$$\left. - \frac{\sinh(\alpha_2 L - \alpha_1 l)}{\alpha_1 - \alpha_2}\right\} - \frac{C_1\beta s^2}{2\alpha_2}\left\{\frac{\cosh(\alpha_2 L + \alpha_1 l)}{\alpha_1 + \alpha_2} + \frac{2\alpha_2 \cosh\left[\alpha_2(L - l)\right]}{\alpha_1^2 - \alpha_2^2}\right.$$

$$\left.\left. - \frac{\cosh(\alpha_2 L - \alpha_1 l)}{\alpha_1 - \alpha_2}\right\} + \left(\alpha_2 \sinh(\alpha_2 L) - C_1 \cosh(\alpha_2 L)\right)\right) \tag{17}$$

where for sinusoidal steady state $V(o, s) = sU(o, s)$, and

$$\beta = \frac{\gamma}{sV(0, s)} = \frac{\gamma}{s^2 U(0, s)} = \frac{\nu R \rho}{E \tau g \cosh(\alpha_1 l)} \tag{18}$$

Transfer Function

The desired transfer function can now be formed from equation (11) by dividing by $U(0, s)$; that is,

$$\frac{U(x, s)}{U(o, s)} = \begin{cases} \dfrac{\beta s^2}{2\alpha_2}\left\{\dfrac{\cosh(\alpha_2 x + \alpha_1 l)}{\alpha_1 + \alpha_2} + \dfrac{2\alpha_2 \cosh\left[\alpha_1(l - x)\right]}{\alpha_1^2 - \alpha_2^2} - \dfrac{\cosh(\alpha_2 x - \alpha_1 l)}{\alpha_1 - \alpha_2}\right\} \\ \qquad + \cosh(\alpha_2 x) + \dfrac{q(s)}{U(0, s)} \dfrac{\sinh(\alpha_2 x)}{\alpha_2} \qquad \text{for } 0 \le x \le l \\ \dfrac{\beta s^2}{2\alpha_2}\left\{\dfrac{\cosh(\alpha_2 x + \alpha_1 l)}{\alpha_1 + \alpha_2} + \dfrac{2\alpha_2 \cosh\left[\alpha_2(l - x)\right]}{\alpha_1^2 - \alpha_2^2} - \dfrac{\cosh(\alpha_2 x - \alpha_1 l)}{\alpha_1 - \alpha_2}\right\} \\ \qquad + \cosh(\alpha_2 x) + \dfrac{q(s)}{U(0, s)} \dfrac{\sinh(\alpha_2 x)}{\alpha_2} \qquad \text{for } l < x \le L \end{cases} \tag{19}$$

where $q(s)/U(0, s)$ is defined by equation (17). For the tank head dynamics, the specialized solution for $x = L$ becomes

$$\frac{U(L, s)}{U(0, s)} = \frac{\beta s^2}{2\alpha_2}\left\{\frac{\cosh(\alpha_2 L + \alpha_1 l)}{\alpha_1 + \alpha_2} + \frac{2\alpha_2 \cosh\left[\alpha_2(L - l)\right]}{\alpha_1^2 - \alpha_2^2} - \frac{\cosh(\alpha_2 L - \alpha_1 l)}{\alpha_1 - \alpha_2}\right\}$$

$$+ \cosh(\alpha_2 L) + \frac{q(s)}{U(0, s)} \frac{\sinh(\alpha_2 L)}{\alpha_2} \tag{20}$$

This equation relates the tank head response to tank base input. Equation (19) and the special case equation (20) are the central result of the analysis.

Resonant Frequency Analysis

It is of some interest to identify the resonant frequencies of the head motion relative to the base. Considering the undamped case only ($K^* = 0$, $K_1 = 0$) the resonant conditions can be found by the roots of the denominators of the various terms of equation (20).

Only two terms of equation (20) yield meaningful results. Setting the denominator of β (eq. (18)) equal to zero gives

$$\cosh \alpha_1 l = \cosh csl = 0 \tag{21}$$

Replacing s with $i\omega$ gives

$$\cos c\omega l = 0$$

which requires

$$\left.\begin{aligned} \omega_n &= \left(\frac{2n - 1}{2}\right)\frac{\pi}{cl} \\ &\text{or} \\ f_n &= \frac{n - \frac{1}{2}}{2cl} \end{aligned}\right\} \tag{22}$$

which are the modes associated with the fluid resonances (ref. 7).

Considering the denominator of the term $q(s)/U(0, s)\left[\sinh(\alpha_2 L)/\alpha_2\right]$ gives (where $q(s)/U(o, s)$ is defined by eq. (17))

$$\frac{C_1 \sinh(\alpha_2 L)}{\alpha_2} - \cosh(\alpha_2 L) = 0 \tag{23}$$

or

$$C_1 \sinh\left(\sqrt{\frac{m_s}{D}}\, sL\right) = \sqrt{\frac{m_s}{D}}\, s \cosh\left(\sqrt{\frac{m_s}{D}}\, sL\right) \tag{24}$$

Now, since C_1 is a function of s and involves the mechanical impedance, the case of a single rigid mass head will be considered (i. e., $Z_m = Ms$). Then,

$$C_1 = -\frac{Ms^2(1-\nu^2)}{2\pi R\tau E} = -C_2 s^2 \tag{25}$$

where

$$C_2 = \frac{M(1-\nu^2)}{2\pi R\tau E} \tag{26}$$

These results substituted into equation (24) with $s = i\omega$ give

$$C_2\omega^2 \sinh\left(\sqrt{\frac{m_s}{D}}\,\omega Li\right) = \sqrt{\frac{m_s}{D}}\,\omega i \cosh\left(\sqrt{\frac{m_s}{D}}\,\omega Li\right)$$

After some manipulation we obtain the result

$$\tan Y = \frac{C_3}{Y} \tag{27}$$

where

$$Y = \sqrt{\frac{m_s}{D}}\,L\omega$$

and

$$C_3 = \frac{m_s L}{DC_2} = \frac{\text{Shell mass}}{\text{Head mass}} \tag{28}$$

Hence the mechanical resonances of the head are given by

$$f_n = \frac{Y_n}{2\pi L\sqrt{\frac{m_s}{D}}} \tag{29}$$

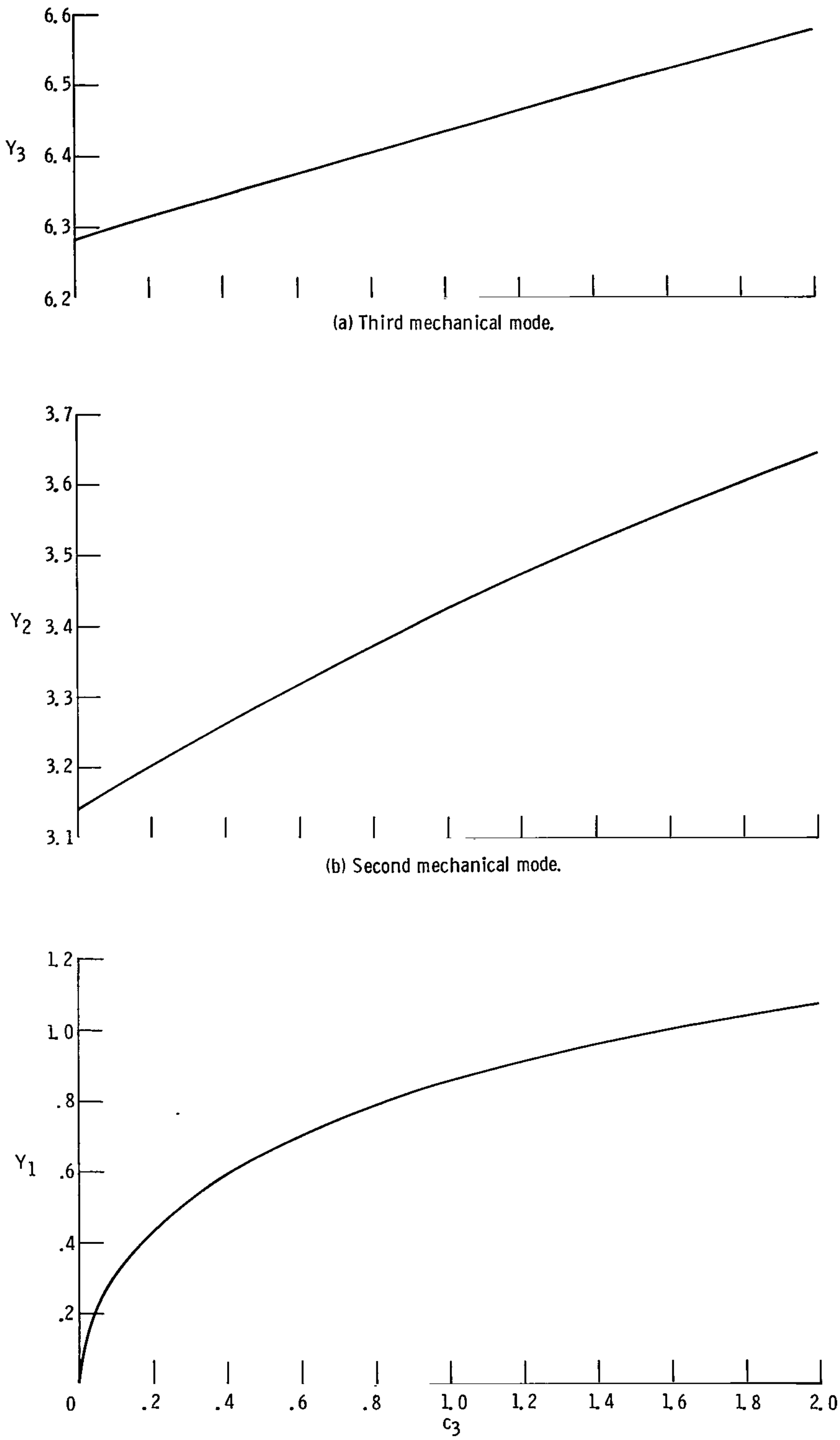

Figure 3. - Parameters for mechanical resonance prediction. Tan $Y = c_3/Y$.

where Y_n are the solutions of equation (27). The mechanical resonances can be identified by equation (29) and the solutions of equation (27) for Y_n. Plots of these solutions are presented in figure 3.

Several refinements can be made for this type of analysis. First, the effect of variation of acoustic velocity with distance can be accounted for. Acoustic velocity varies with distance because the end plates restrain the shell motion and thereby effectively increase acoustic velocity in that area. When accounting for the variation in wave propagation time it is expected that the fluid resonant frequencies with variable acoustic velocity would be given by

$$f_n = \frac{n - \frac{1}{2}}{2 \int_0^l c(x)dx}$$

The variation of c (local reciprocal acoustic velocity) with axial distance x can be expressed as

$$c(x) = \sqrt{\frac{p}{g}\left(B + \frac{2}{R}\frac{\partial R}{\partial p}\right)} \tag{31}$$

where the symbols are as defined earlier.

The volume change due to shell bending can be calculated from classical shell theory (ref. 12, p. 36). For example, the solution for a cylindrical shell with the boundary conditions

$$\left.\begin{aligned} x = 0 \rightarrow w = 0 \qquad &\text{and} \qquad \frac{dw}{dx} = 0 \\ x = L \rightarrow w = 0 \qquad &\text{and} \qquad \frac{dw}{dx} = 0 \end{aligned}\right\} \tag{32}$$

is

$$\frac{2}{R}\frac{\partial R}{\partial p} = \frac{2R}{E\tau} - \left(\frac{2\psi}{R} \sin \varphi y \sinh \varphi y + \frac{2\lambda}{R} \cos \varphi y \cosh \varphi y\right) \tag{33}$$

where

$$\left.\begin{aligned}
\psi &= \frac{2R^2}{E\tau}\left(\frac{\sin\alpha\cosh\alpha - \cos\alpha\sinh\alpha}{\sin 2\alpha + \sinh 2\alpha}\right) \\
\lambda &= \frac{2R^2}{E\tau}\left(\frac{\cos\alpha\sinh\alpha + \sin\alpha\cosh\alpha}{\sin 2\alpha + \sinh 2\alpha}\right) \\
\alpha &= \frac{\varphi L}{2} \\
\varphi^4 &= \frac{3(1 - \nu^2)}{R^2\tau^2} \\
y &= x - \frac{L}{2}
\end{aligned}\right\} \tag{34}$$

Basically only the ends of the tank are influenced by this variation of c with length.

A second refinement would be the inclusion of acoustic modes in the ullage gas. The frequencies of these modes are predicted by the equation

$$f_{n,a} = \frac{na}{2(L - l)} \tag{35}$$

where a is the acoustic velocity in the gas column and $(L - l)$ is the gas column length. These gas column acoustic modes have a very narrow band width and when tuned with a fluid mode tend to depress it (ref. 13). It appeared that inclusion of this type mode in the analysis was inconsistent with the objectives of the present work.

EXPERIMENTAL STUDY

An experimental study was conducted to serve as a basis of comparison with the analysis. The test specimen was a cylindrical Plexiglas tank having a fixed rigid base and a removable rigid head. Plexiglas was chosen so that the fluid surface modes might be observed and for ease of fabrication.

The salient characteristics of the tank are as follows:

Outside diameter, in. (m)	18 (0.457)
Wall thickness, in. (m)	1/8 (0.003175)
Inside length, in. (m)	38.75 (0.984)
Overall height, in. (m)	44.0 (1.115)
Weight of base and tube, lbm (kg)	86.31 (39.1)
Weight of head, hardware, and instrumentation, lbm (kg)	28.0 (12.7)
Density, $\mathrm{lbm/ft^3}$ ($\mathrm{kg/m^3}$)	74.3 (11 850)
Material	Plexiglas

The tank is shown mounted on a 28 000-pound force (1.25×10^5 Newton) electrodynamic shaker in figure 4. Lateral support was not required with this shaker, nor was a suspension system.

The instrumentation for the tests consisted of 11 piezoelectric accelerometers located to detect longitudinal motion (and 4 accelerometers for lateral motion of head and base). Also, two transducers measured tank base pressure at the center and one-half radius positions.

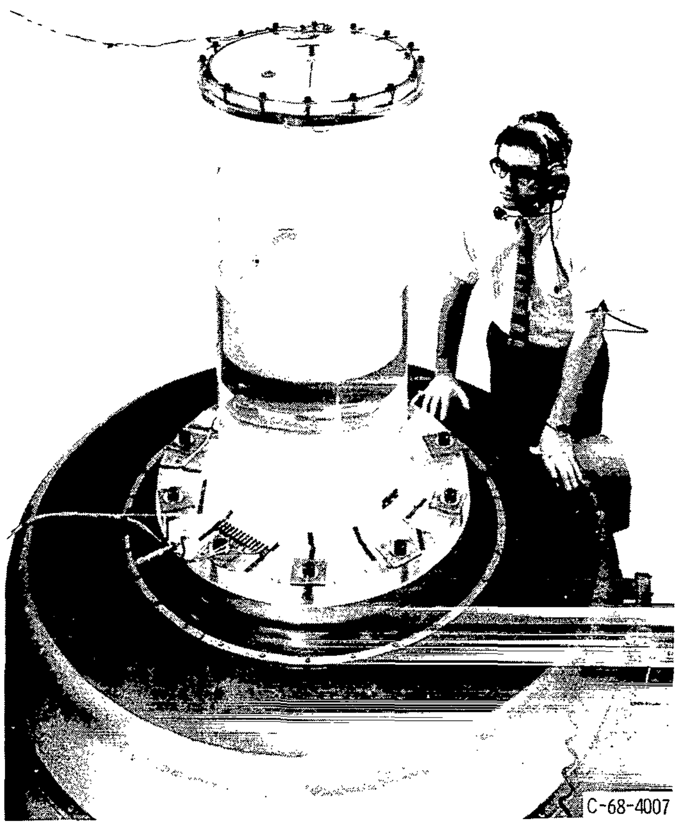

Figure 4. - Plexiglas tank on shaker.

The normal testing procedure was to drive the system sinusoidally maintaining a 1-g base acceleration amplitude (longitudinal) while sweeping from 20 to 400 hertz at a sweep rate of 1 octave per minute. The only variation from this procedure was for the mode shape studies where a selected constant resonant frequency was dwelled on for 20 seconds.

All test data were recorded on magnetic tape and analyzed using analog frequency analysis techniques.

COMPARISON OF ANALYSIS AND EXPERIMENT

The fundamental objective of the study was to predict the head to base transfer function for a cylindrical tank partially filled with fluid. For this configuration the tank base pressure to base acceleration, and tank head acceleration to base acceleration transfer functions were analytically and experimentally determined for each 1/8 fullness point. Several parameters required in the analysis were either unknown or uncertain. The basic unknowns were the distributed damping numbers K^* and K_1 and the reciprocal acoustic velocity of the fluid c.

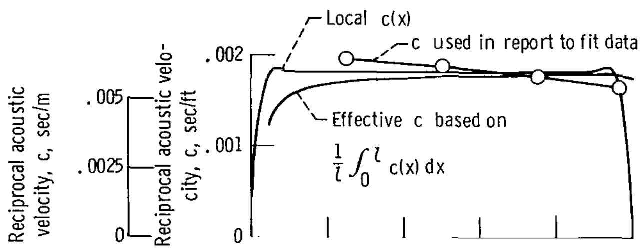

(a) Reciprocal acoustic velocity c as function of nondimensional fluid height l/L.

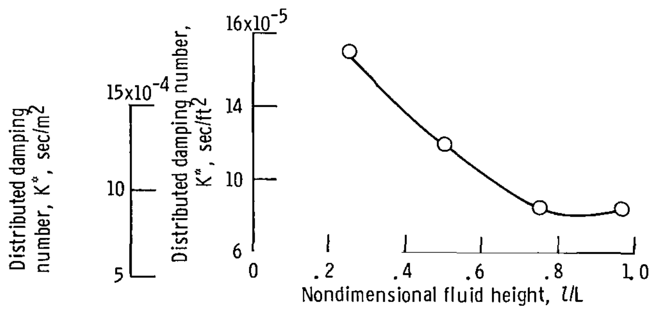

(b) Damping number K* as function of nondimensional fluid height l/L.

Figure 5. - Parameters of analytical model as function of nondimensional fullness.

The difficulty in determining acoustic velocity is two-fold. The projected effects due to end boundary constraints were discussed previously. Secondly, uncertainty in selection of the proper modulus of elasticity from stress-strain diagrams was experienced due to the plastic behavior of the Plexiglas.

For these reasons the fluid reciprocal acoustic velocity c and the distributed damping number K^* were chosen to approximate the fundamental fluid mode as identified on the tank base pressure to tank base acceleration transfer functions.

These parameters and a modulus of elasticity of 8.6×10^7 pounds per square foot (4.12×10^9 N/m^2) based on a mean c value ($c = 0.00181$ sec/ft, 0.00594 sec/m) were then used to predict the head to base transfer functions. For the distributed mechanical damping number a value of $K_1 = 0.000015$ second per square foot (0.1615×10^{-3} sec/m^2) approximated the results for all fullnesses.

The c and K^* values determined by the previous procedure have been plotted against relative fullness (l/L) in figure 5. The effective c of the system (fig. 5(a)) gradually decreases with increasing fluid height. Also shown on the plot is $c(x)$ as predicted by equations (31) to (34) and

$$c_{ef} = \frac{1}{l}\int_0^l c(x)dx$$

In figures 6 to 10, respectively, typical results are presented for the 0, 1/4, 1/2, 3/4, and 0.96 fullness experimental and corresponding analytical transfer functions. The (a) and (b) figures are the head to base transfer function and the (c) and (d) figures are the base pressure to base acceleration transfer function. Mode identification for these plots will be aided by referring ahead to the summary plot figure 13.

While the asymmetric modes were not predicted, the model did a reasonable job of predicting general response amplitude, indicating that the damping form is acceptable. The phase angle was apparently strongly influenced at the higher frequencies by the asymmetric modes. Apparent also in the head response data are the modes associated with the acoustics of the ullage gas. It will be noticed (i.e., 1/4 fullness, fig. 7) that while these modes influence head motion the effects on tank base pressure are minimal.

It is important to note that for some fullness conditions the contribution to the head response by the fluid mode is more important than that of the mechanical mode. This occurs for the quarter full case where the fluid mode ($f = 152$ Hz) has an amplitude ratio of 11 while the mechanical mode ($f = 202$ Hz) is about 5.5. This also occurs for the 5/8 full case (data not presented) where the second fluid mode is dominant over the mechanical mode. This clearly indicates the importance of coupling the fluid behavior to the tank walls for predicting head motion.

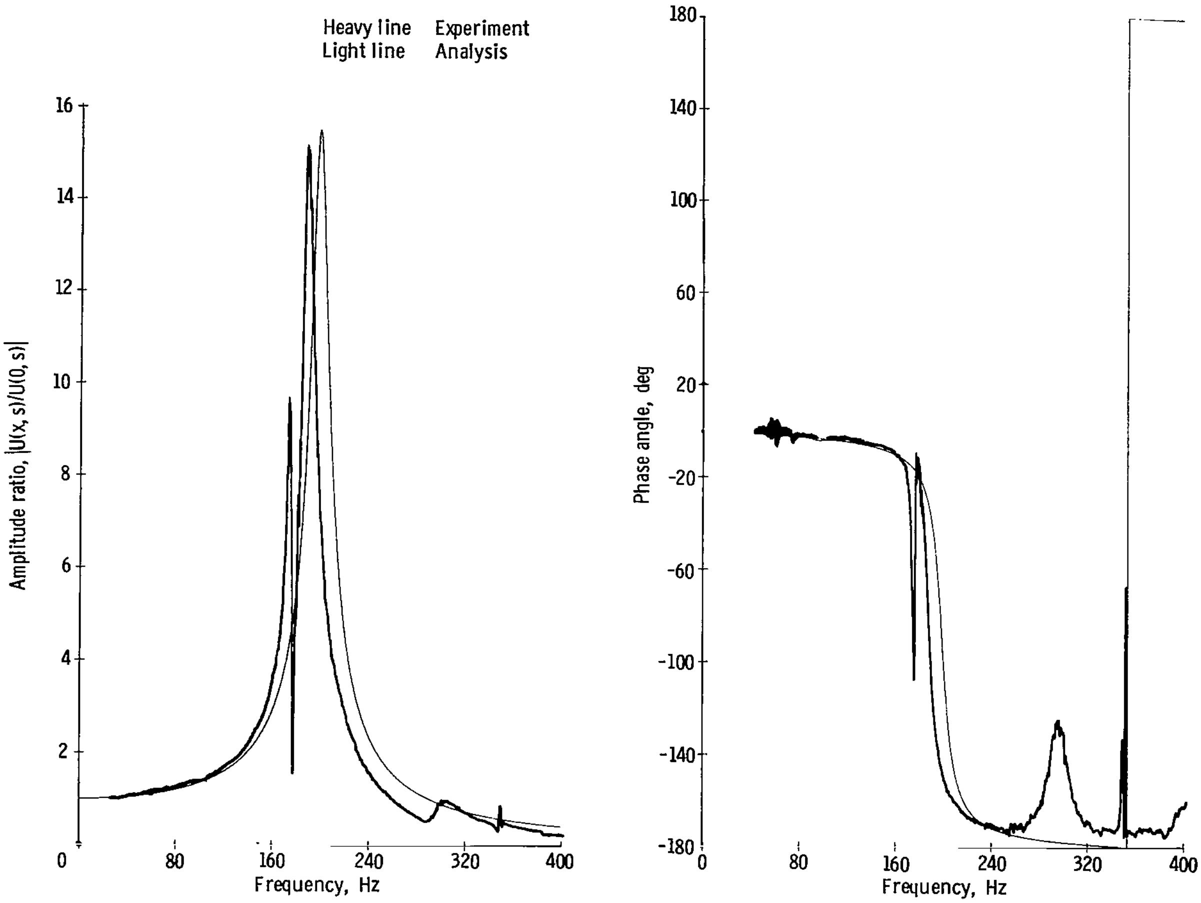

(a) Amplitude ratio.

(b) Phase angle.

Figure 6. - Empty tank head to base response.

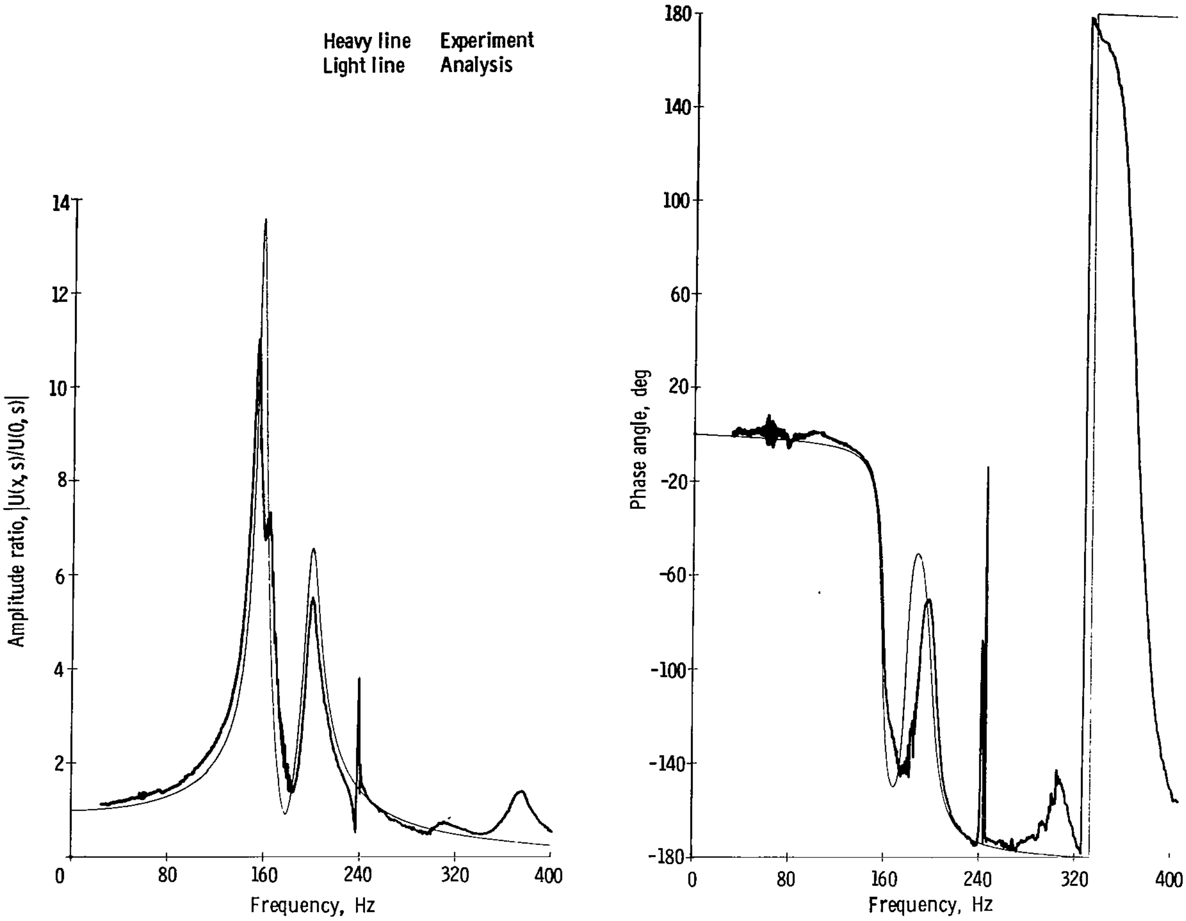

(a) Tank head to base response; amplitude ratio.

(b) Tank head to base response; phase angle.

Figure 7. - One-quarter full tank head to base response.

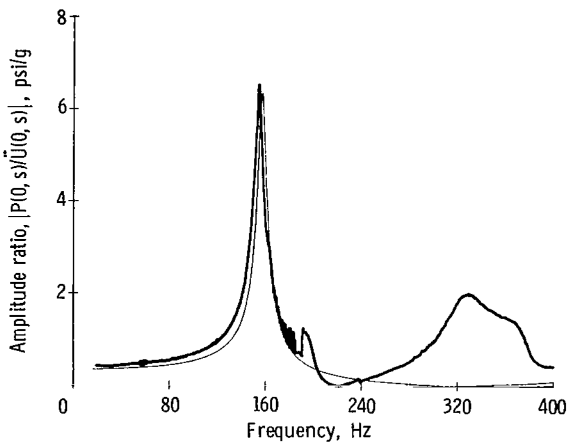

(c) Tank base pressure to tank base acceleration response; amplitude ratio.

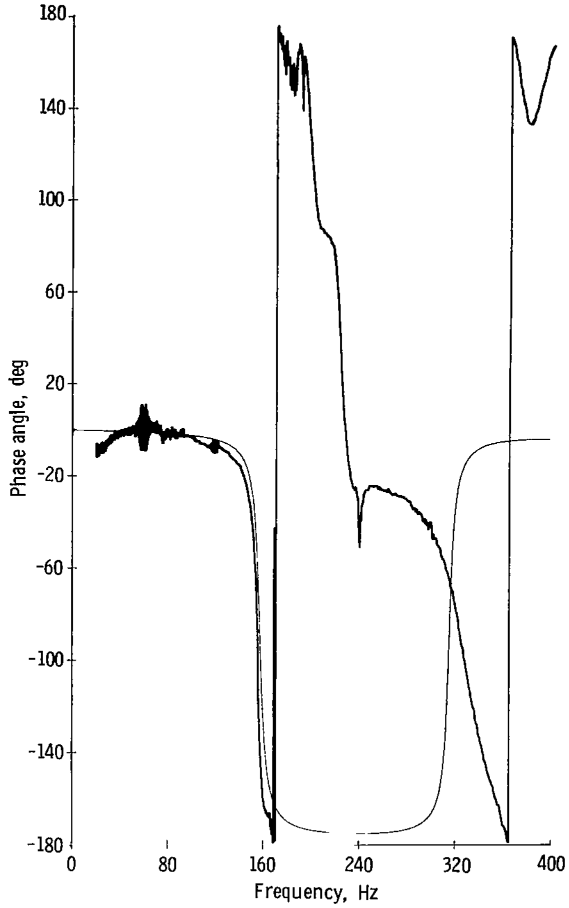

(d) Tank base pressure to tank base acceleration response; phase angle.

Figure 7. - Concluded.

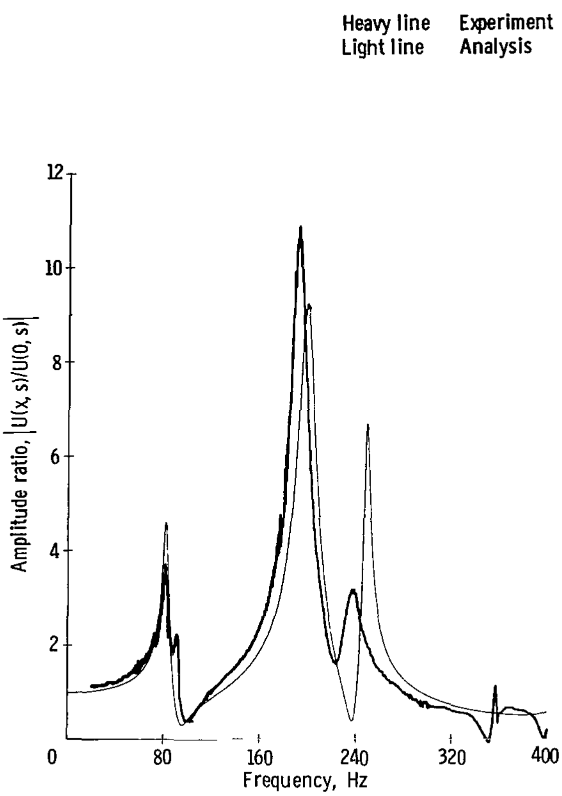

(a) Tank head to base response; amplitude ratio.

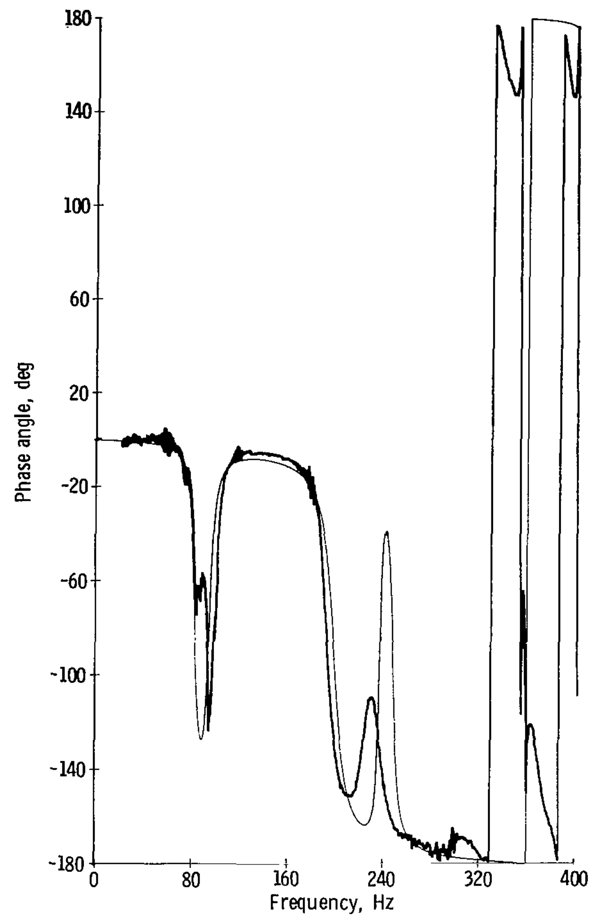

(b) Tank head to base response; phase angle.

Figure 8. - One-half full tank head to base response.

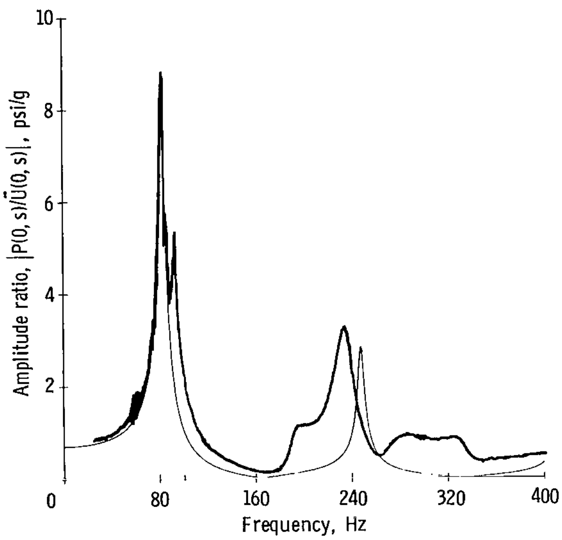

(c) Tank base pressure to tank base acceleration response; amplitude ratio.

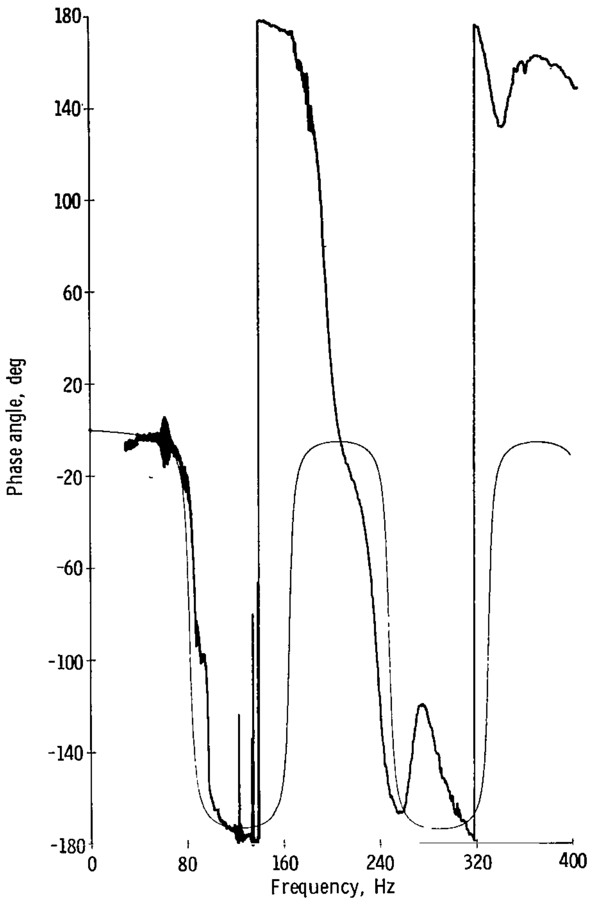

(d) Tank base pressure to tank base acceleration response; phase angle.

Figure 8. - Concluded.

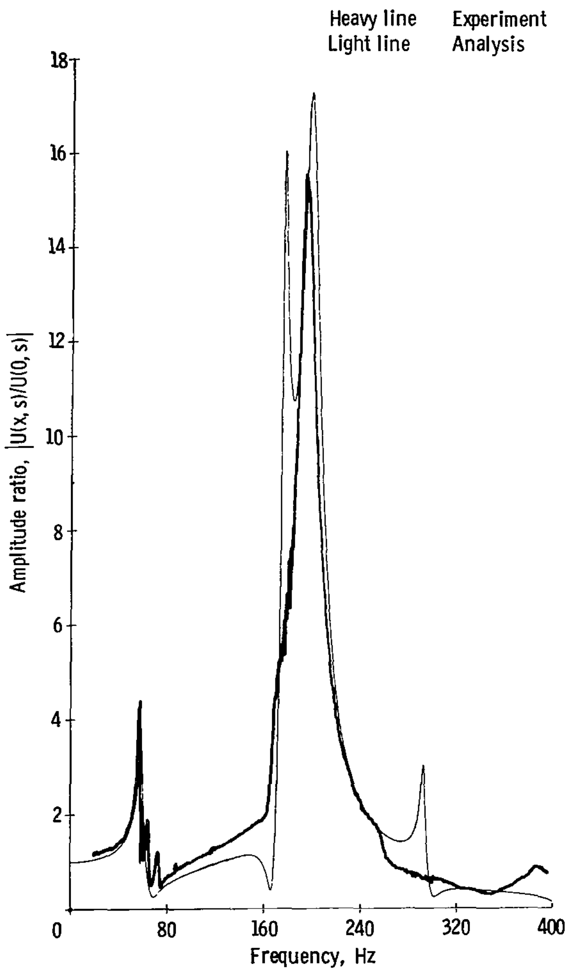

(a) Tank head to base response; amplitude ratio.

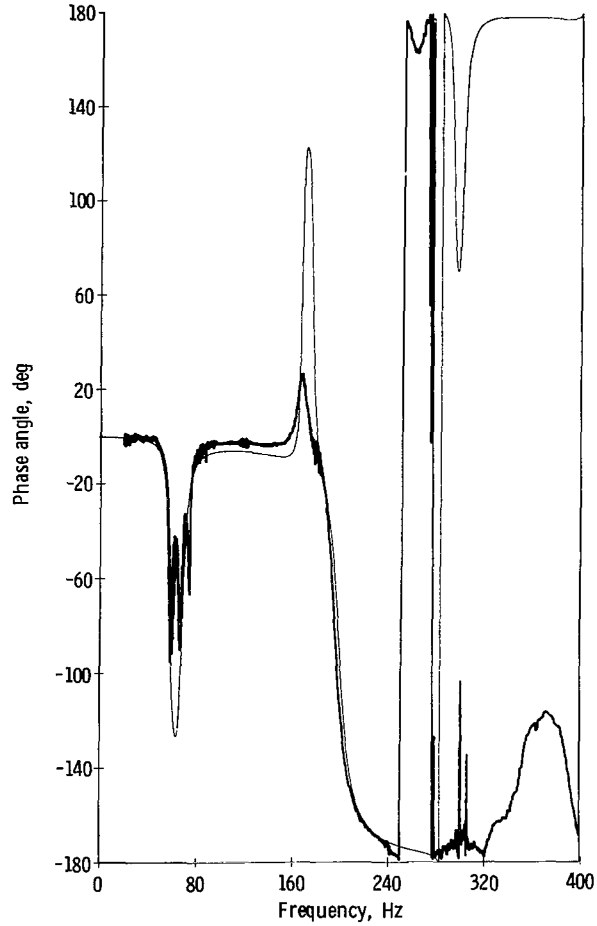

(b) Tank head to base response; phase angle.

Figure 9. - Three-quarters full tank head to base response.

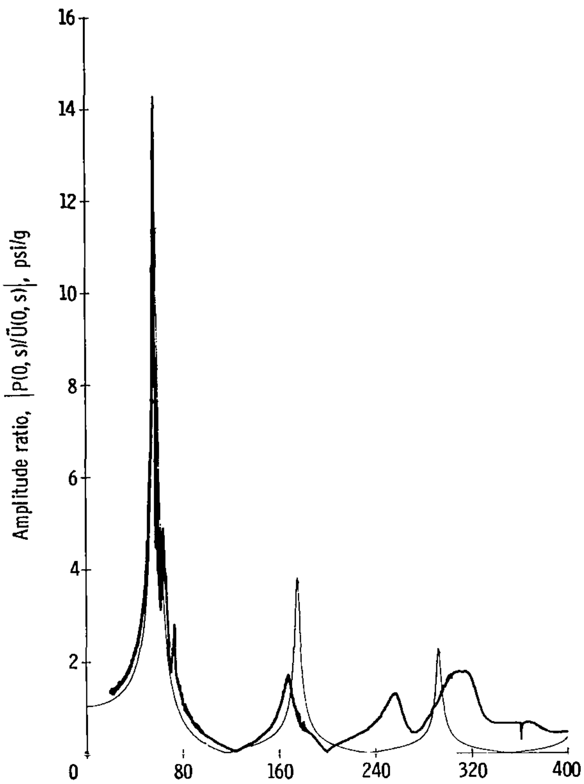

(c) Tank base pressure to tank base acceleration response; amplitude ratio.

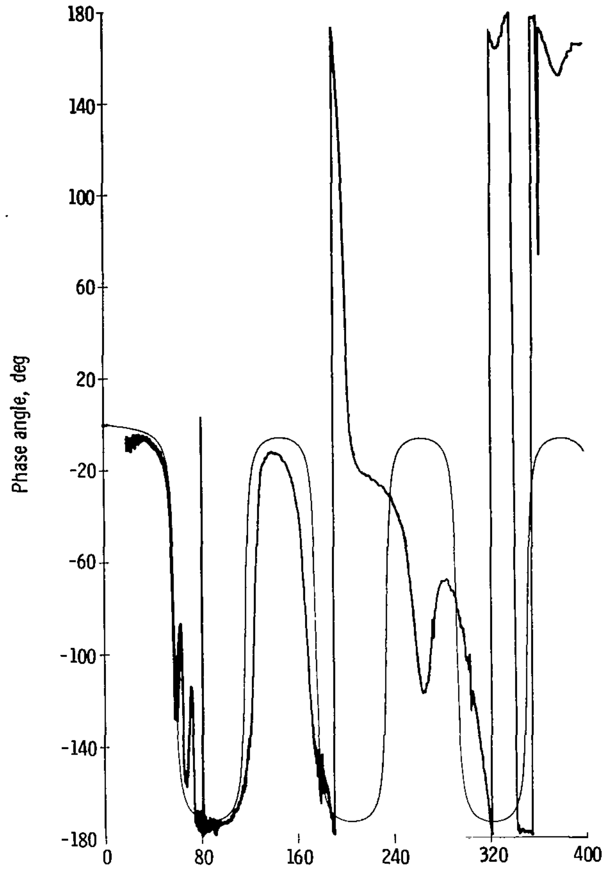

(d) Tank base pressure to tank base acceleration response; phase angle.

Figure 9. - Concluded.

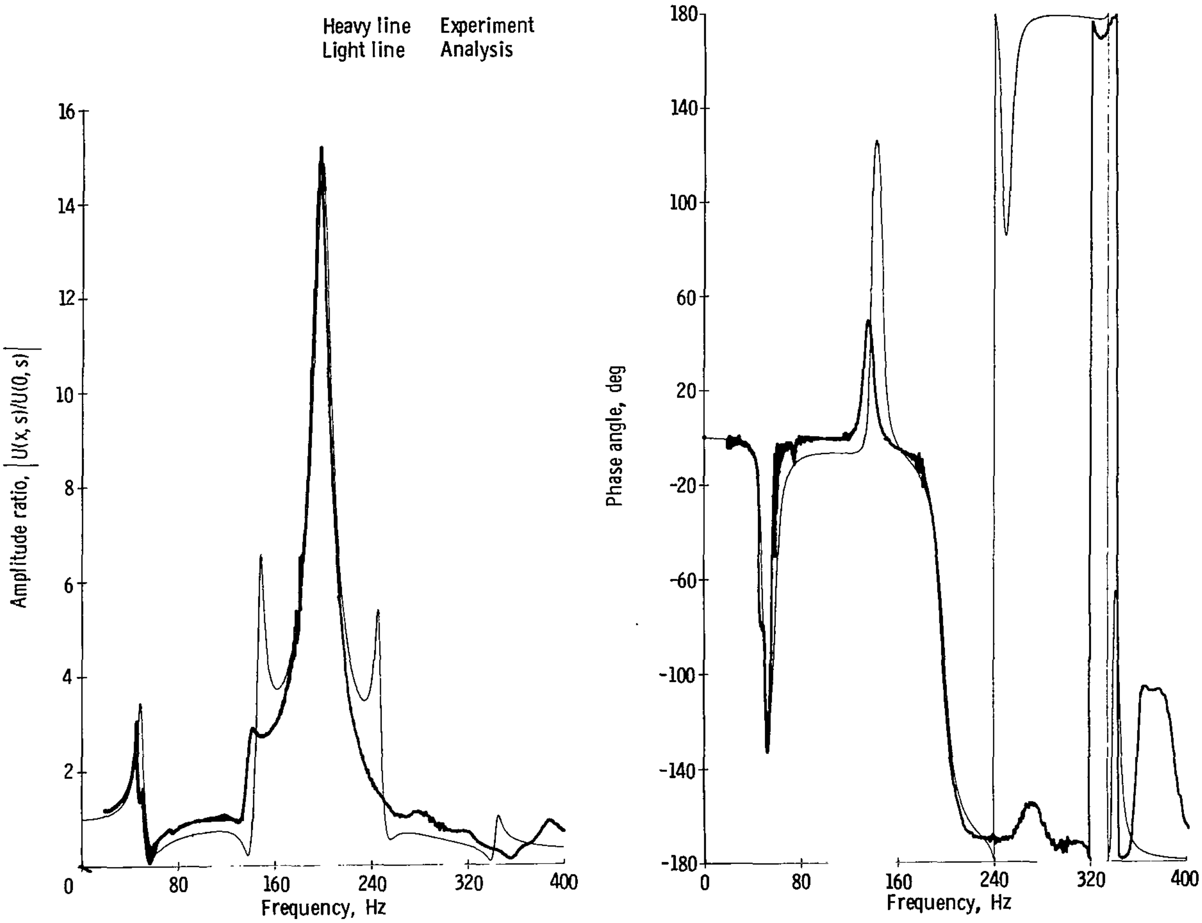

(a) Tank head to base response; amplitude ratio.

(b) Tank head to base response; phase angle.

Figure 10. - Full tank head to base response.

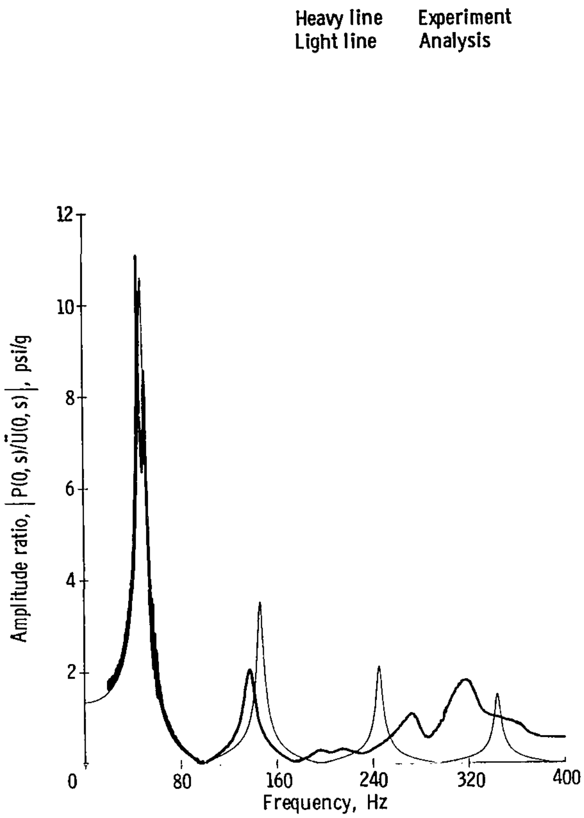

(c) Tank base pressure to tank base acceleration response; amplitude ratio.

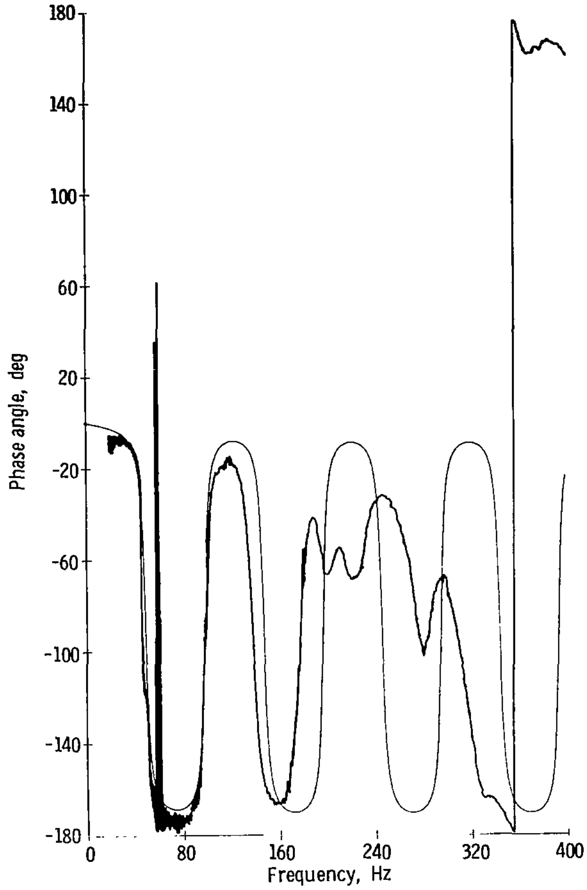

(d) Tank base pressure to tank base acceleration response; phase angle.

Figure 10. - Concluded.

It is also of interest to note for the 3/4 full case the coalescence of the second fluid mode and the head mechanical mode for the experiment while two separate resonances showed for the model. The model resonance would coalesce at a slightly less full condition or with a small shift in acoustic velocity.

A comparison of the fluid acoustic velocity assumptions is made in figure 11. Here, the fundamental fluid mode frequency is plotted against nondimensional fluid height for the constant and variable reciprocal acoustic velocity cases and the experiment. Either approximation is quite good for $l/L > 0.35$. At this fluid height the wave length,

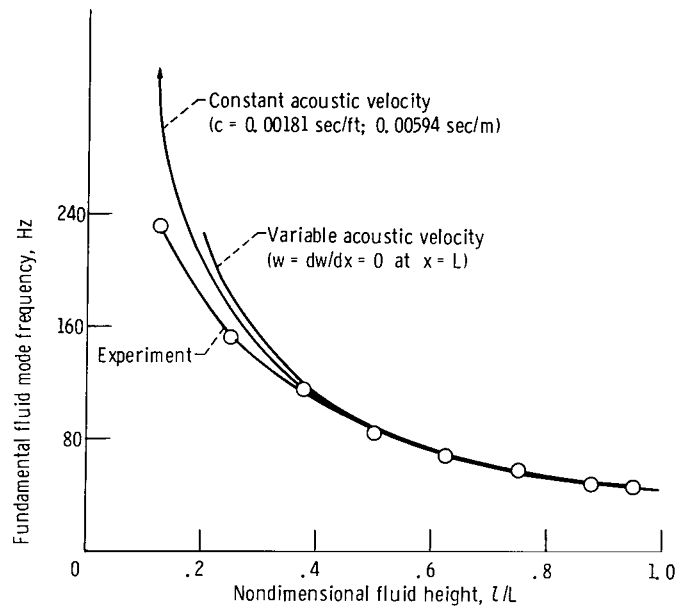

Figure 11. - Comparison of experimental and analytical fundamental fluid mode frequencies.

based on c = 0.00181 second per foot (0.00594 sec/m), is equal to the tank circumference; under such conditions the acoustic scattering becomes significant (ref. 4, p. 350), distorting and interfering with plane wave propagation.

For an acoustic velocity of 1135 feet per second (346 m/sec) in the air above the liquid the frequencies of the gas column acoustic modes as predicted by equation (35) are plotted in figure 12 along with the experimentally observed modes.

A summary of the experimentally observed resonant frequencies as a function of fullness is presented in figure 13. Identified on this plot are the fluid modes, the mechanical head modes, and the ullage gas modes.

Typical experimental modes shape plots generated by driving at the resonant frequencies are presented in figure 14 for the 3/4 full case. Here, shell longitudinal

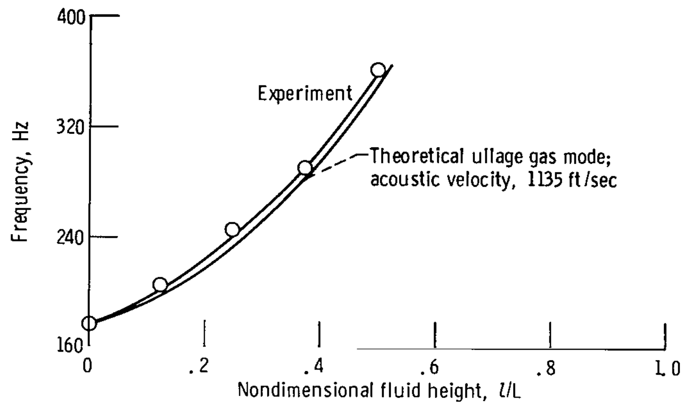

Figure 12. - Comparison of experimental and analytical ullage gas mode frequencies.

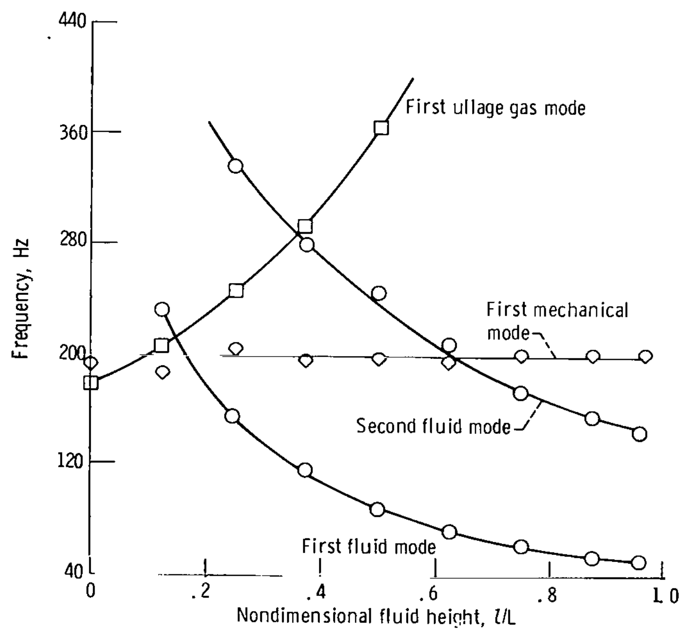

Figure 13. - Summary plot - experimental resonant frequencies as function of fullness.

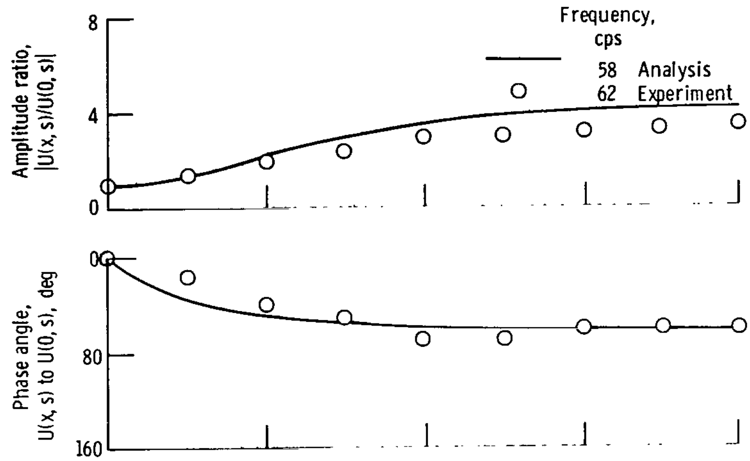

(a) Fluid fundamental mode.

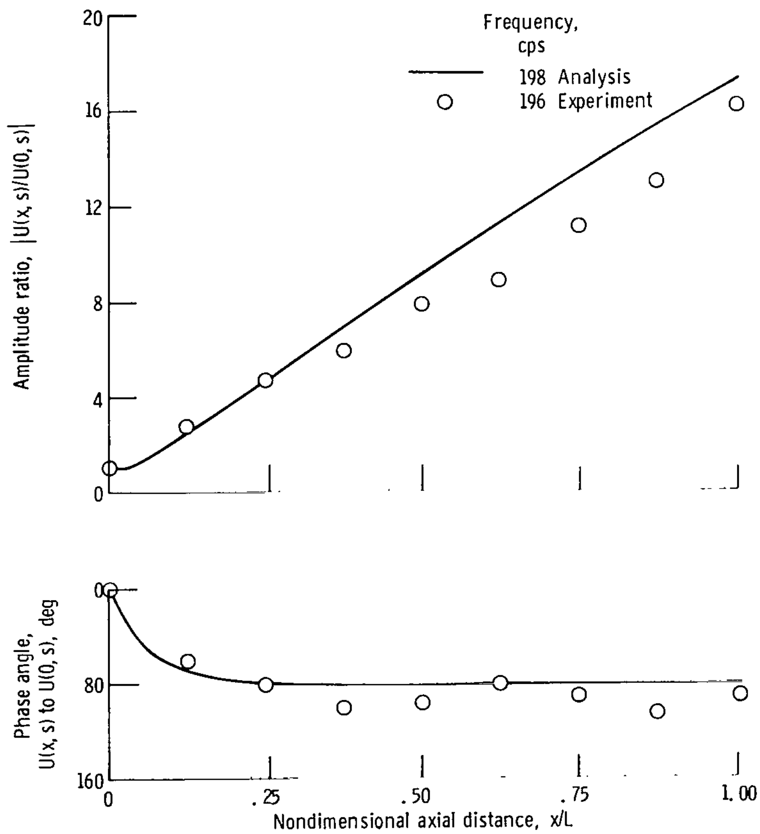

(b) Mechanical mode.

Figure 14. - Shell longitudinal mode shape for 3/4 full tank.

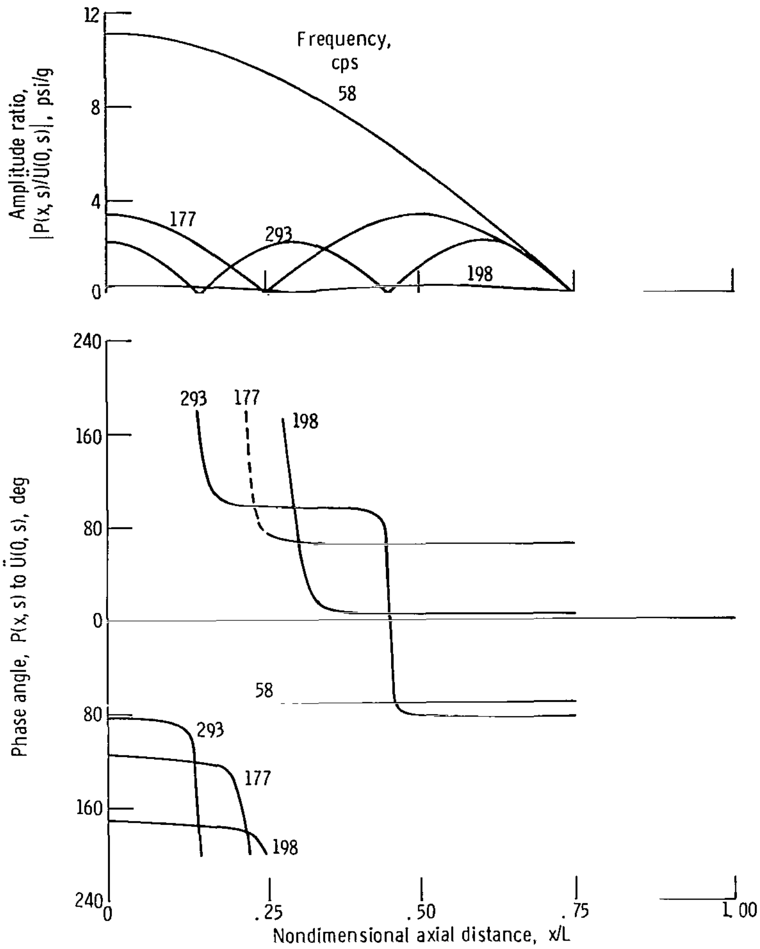

Figure 15. - Analytical pressure to base acceleration mode shape for 3/4 full tank.

acceleration at a given x-position to base acceleration, amplitude and phase is plotted against tank length. Also presented are the corresponding analytical results. The agreement between the two is good. The pressure to base acceleration mode shape was not measured in the experiment; however, the analytical values for these are presented in figure 15.

CONCLUSIONS

1. A model has been developed which predicts the head to base transfer function for a cylindrical tank partially filled with fluid. The model yields closed form results and accounts for the influence of fluid pressure effects and distributed mechanical and fluid damping.

2. The model did an adequate job of matching the transfer functions and mode shapes consistent with the objectives of the study.

3. There remains some question as to proper choice of reciprocal acoustic velocity c and its variation with the x coordinate and fluid height. However, constant c values should be satisfactory. Also the distributed damping numbers K_1 and K^* must be determined.

4. The results clearly demonstrate the importance of considering fluid resonance effects on head to base response. Indeed in at least two cases the fluid mode effects dominated the mechanical modes for this transfer function.

Lewis Research Center,
National Aeronautics and Space Administration,
Cleveland, Ohio, March 16, 1970,
124-09.

APPENDIX A

SYMBOLS

A	area, ft^2 (m^2)
a	acoustic velocity, ft/sec (m/sec)
B	fluid compressibility, ft^2/lb (m^2/N)
c	reciprocal acoustic velocity, sec/ft (sec/m)
c_1	function of s, see eq. (25)
c_2	constant, see eq. (26)
c_3	constant, see eq. (28)
D	rigidity of the shell, $E\tau/(1 - \nu^2)$, lb/ft (N/m)
E	modulus of elasticity, lb/ft^2 (N/m^2)
F	force, lb (N)
f	frequency, Hz
g	gravitational constant, ft/sec^2 (m/sec^2)
H	function defined by eq. (7)
K	proportionality constant per unit length for fluid damping, lb-sec/ft^2 (N-sec/m^2)
K^*	distributed fluid damping, $(K/A)\left[B + (2R/E\tau)\right]$, sec/$ft^2$
K_1	distributed mechanical damping, sec/ft^2 (sec/m^2)
L	tank height, ft (m)
$\mathscr{L}$	Laplace transform operator with respect to t
x	Laplace transform operator with respect to x
l	height of fluid in tank, ft (m)
M	head mass, slugs (kg)
m_s	mass per unit area of shell, $\rho_w\tau/g$, lb-sec^2/ft^3 (N-sec^2/m^3)
n	mode number, integer
p	pressure, lb/ft^2 (N/m^2)
$\wp$	Laplace variable with respect to distance x, 1/ft (1/m)
q	$dU(0^+, s)/dx$
R	radius, ft (m)

$\mathcal{S}$	unit step function
s	Laplace variable with respect to time, 1/sec
t	time, sec
u	displacement, ft (m)
v	velocity, ft/sec (m/sec)
w	radial displacement, ft (m)
x	distance coordinate, ft (m)
Y	$\sqrt{m_s/D}\, L\omega$, rad
y	distance coordinate from center of tank, ft (m)
Z_m	mechanical impedance, lb-sec/ft (N-sec/m)
Z_1, Z_2	dummy variables for hyperbolic identify
α	$\varphi L/2$
α_1	$\sqrt{c^2 s^2 + K^* s}$, 1/ft (1/m)
α_2	$\sqrt{(m_s/D)s^2 + K_1 s}$, 1/ft (1/m)
β	$\gamma/sv(0,s)$, see eq. (18), sec^2/ft^2 (sec^2/m^2)
γ	$(\rho R\nu/E\tau g)\left[sV(0,s)/\cosh(\alpha_1 l)\right]$, 1/ft (1/m)
λ	variable defined by eq. (34)
ν	Poisson ratio
ξ	dummy variable
ρ	density, lb/ft^3 (kg/m^3)
τ	wall thickness, ft (m)
φ	$\sqrt[4]{\dfrac{3(1-\nu^2)}{R^2\tau^2}}$, 1/ft (1/m)
ψ	variable defined by eq. (34)
ω	angular frequency, rad/sec

Subscripts:

a	acoustic mode
n	mode number, integer
ef	effective

x with respect to x

w wall

For variables U, P, H, V, and W, lower case represents the untransformed variable. Upper case represents variable transformed with respect to t, and script represents variable transformed with respect to both t and x.

APPENDIX B

INVERSE TRANSFORM CALCULATION

To find the inverse Laplace transform with respect to x of equation (10),

$$\mathscr{U}(p, s) = \frac{\mathscr{H}(p, s) + pU(o, s) + q(s)}{p^2 - \left(K_1 s + \frac{m_s}{D} s^2\right)}$$

$\mathscr{U}(p, s)$ will be considered in three parts; namely,

$$\mathscr{U}_1(p, s) = \frac{\mathscr{H}(p, s)}{p^2 - \left(K_1 s + \frac{m_s}{D} s^2\right)} \tag{B1}$$

$$\mathscr{U}_2(p, s) = \frac{pU(o, s)}{p^2 - \left(K_1 s + \frac{m_s}{D} s^2\right)} \tag{B2}$$

and

$$\mathscr{U}_3(p, s) = \frac{q(s)}{p^2 - \left(K_1 s + \frac{m_s}{D} s^2\right)} \tag{B3}$$

Equation (7) can be rewritten as

$$H(x, s) = H_1(x, s)\left[1 - \mathscr{S}(x - l)\right] \tag{B4}$$

where

$$H_1(x, s) = \left[\left(\frac{\nu R \rho}{E \tau g}\right) \frac{sV(0, s)}{\cosh\left(\sqrt{c^2 s^2 + K^* s}\, l\right)}\right] \cosh\left[\sqrt{c^2 s^2 + K^* s}\,(l - x)\right] \tag{B5}$$

The inverse of $\mathscr{U}_1(p, s)$ then can be expressed as

$$U_1(x, s) = \mathscr{L}_x^{-1}\left\{\frac{\mathscr{L}_x H_1(x, s)\left[1 - \mathscr{S}(x - l)\right]}{p^2 - \left(K_1 s + \frac{m_s}{D} s^2\right)}\right\} \tag{B6}$$

Making the substitutions

$$\left.\begin{aligned} \alpha_1 &= \sqrt{c^2 s^2 + K^* s} \\ \alpha_2 &= \sqrt{\frac{m_s}{D} s^2 + K_1 s} \\ \gamma &= \frac{\nu R \rho}{E \tau g} \frac{sV(o, s)}{\cosh(\alpha_1)} \end{aligned}\right\} \tag{B7}$$

and applying the convolution theorem to equation (B6) give

$$U_1(x, s) = \int_0^x \gamma \cosh\left[\alpha_1(l - \xi)\right]\left[1 - \mathscr{S}(\xi - l)\right] \frac{1}{\alpha_2} \sinh\left[\alpha_2(x - \xi)\right] d\xi \tag{B8}$$

$$U_1(x, s) = \begin{cases} \displaystyle\int_0^x \frac{\gamma}{\alpha_2} \cosh\left[\alpha_1(l - \xi)\right]\sinh\left[\alpha_2(x - \xi)\right] d\xi & \text{for } 0 \leq x \leq l \\ \displaystyle\int_0^l \frac{\gamma}{\alpha_2} \cosh\left[\alpha_1(l - \xi)\right]\sinh\left[\alpha_2(x - \xi)\right] d\xi & \text{for } x \geq l \end{cases}$$

Using the hyperbolic identity

$$\sinh Z_1 \cosh Z_2 = \frac{1}{2}\sinh(Z_1 + Z_2) + \frac{1}{2}\sinh(Z_1 - Z_2)$$

and performing the required integrations give

$$U_1(x, s) = \begin{cases} \dfrac{\gamma}{2\alpha_2}\left\{-\dfrac{\cosh\left[\alpha_1(l - x)\right]}{\alpha_1 + \alpha_2} + \dfrac{\cosh(\alpha_2 x + \alpha_1 l)}{\alpha_1 + \alpha_2} + \dfrac{\cosh\left[\alpha_1(x - l)\right]}{\alpha_1 - \alpha_2} - \dfrac{\cosh(\alpha_2 x - \alpha_1 l)}{\alpha_1 - \alpha_2}\right\} & \text{for } 0 \leq x \leq l \\[2ex] \dfrac{\gamma}{2\alpha_2}\left\{-\dfrac{\cosh\left[\alpha_2(x - l)\right]}{\alpha_1 + \alpha_2} + \dfrac{\cosh(\alpha_2 x + \alpha_1 l)}{\alpha_1 + \alpha_2} + \dfrac{\cosh\left[\alpha_2(x - l)\right]}{\alpha_1 - \alpha_2} - \dfrac{\cosh(\alpha_2 x - \alpha_1 x)}{\alpha_1 - \alpha_2}\right\} & \text{for } x \geq l \end{cases} \tag{B9}$$

The inverse transform of equation (B2) with respect to x is readily found as

$$U_2(x, s) = U(0, s)\cosh(\alpha_2 x) \tag{B10}$$

To obtain the inverse transform of equation (B3) it is noted that the unknown q is only a function of s; hence,

$$U_3(x, s) = q(s)\,\frac{1}{\alpha_2}\sinh(\alpha_2 x) \tag{B11}$$

Combining the results of equations (B9), (B10), and (B11) gives the inverse transform of equation (10) as

$$U(x, s) = \begin{cases} \dfrac{\gamma}{2\alpha_2}\left\{\dfrac{\cosh(\alpha_2 x + \alpha_1 l)}{\alpha_1 + \alpha_2} - \dfrac{\cosh\left[\alpha_1(l - x)\right]}{\alpha_1 + \alpha_2} + \dfrac{\cosh\left[\alpha_1(x - l)\right]}{\alpha_1 - \alpha_2} - \dfrac{\cosh(\alpha_2 x - \alpha_1 l)}{\alpha_1 - \alpha_2}\right\} & \\ \qquad + U(0, s)\cosh(\alpha_2 x) + \dfrac{q(s)}{\alpha_2}\sinh(\alpha_2 x) & \text{for } 0 \leq x \leq l \\[2ex] \dfrac{\gamma}{2\alpha_2}\left\{\dfrac{\cosh(\alpha_2 x + \alpha_1 l)}{\alpha_1 + \alpha_2} - \dfrac{\cosh\left[\alpha_2(x - l)\right]}{\alpha_1 + \alpha_2} + \dfrac{\cosh\left[\alpha_2(x - l)\right]}{\alpha_1 - \alpha_2} - \dfrac{\cosh(\alpha_2 x - \alpha_1 l)}{\alpha_1 - \alpha_2}\right\} & \\ \qquad + U(0, s)\cosh(\alpha_2 x) + \dfrac{q(s)}{\alpha_2}\sinh(\alpha_2 x) & \text{for } l \leq x \leq L \end{cases} \tag{B12}$$

where

$$\alpha_1 = \sqrt{c^2 s^2 + K^* s}$$

$$\alpha_2 = \sqrt{\frac{m_s}{D} s^2 + K_1 s}$$

$$\gamma = \frac{\nu R \rho}{E \tau g} \frac{sV(o, s)}{\cosh(\alpha_1 l)}$$

At the tank top ($x = L > l$)

$$U(L, s) = \frac{\gamma}{2\alpha_2}\left\{\frac{\cosh(\alpha_2 L + \alpha_1 l)}{\alpha_1 + \alpha_2} + \frac{2\alpha_2 \cosh\left[\alpha_2 (L - l)\right]}{\alpha_1^2 - \alpha_2^2} - \frac{\cosh(\alpha_2 L - \alpha_1 l)}{\alpha_1 - \alpha_2}\right\}$$

$$+ U(o, s)\cosh(\alpha_2 L) + \frac{q(s)}{\alpha_2} \sinh(\alpha_2 L) \qquad \text{for } x = L \qquad \text{(B13)}$$

REFERENCES

1. Rubin, Sheldon: Longitudinal Instability of Liquid Rockets Due to Propulsion Feedback (POGO). J. Spacecraft Rockets, vol. 3, no. 8, Aug. 1966, pp. 1188-1195.

2. Meisenholder, S. G.; and Bickford, L. L.: "POGO" Analysis of the Saturn Propulsion System. Rep. AMDR-9635-037, Aerojet-General Corp. (NASA CR-86432), Apr. 3, 1967.

3. Rose, Robert G.; Simson, Anton K.; and Staley, James A.: A Study of System-Coupled Longitudinal Instabilities in Liquid Rockets. Part 1: Analytic Model. Rep. GD/C-DDE65-049, pt. 1, General Dynamics/Convair (AFRPL-TR-65-163, pt. 1, DDC No. AD-471523), Sept. 1965.

4. Rose, Robert G.; Simson, Anton K.; and Staley, James A.: A Study of System-Couples Longitudinal Instabilities in Liquid Rockets. Part 2: Computer Program. Rep. GD/C-DDE65-049, pt. 2, General Dynamics/Convair (AFRPL-TR-65-163, pt. 2, DDC No. AD-471508), Sept. 1965.

5. Wood, John D.: Survey on Missile Structural Dynamics. Rep. EM-11-11, Space Technology Labs., Inc. (BSD-TN-61-42), June 1, 1961.

6. Pinson, Larry D.: Longitudinal Spring Constants for Liquid-Propellant Tanks with Ellipsoidal Ends. NASA TN D-2220, 1964.

7. Lorenzo, Carl F.: Transfer Function Analysis of a Fluid Contained in a Longitudinally Excited Thin-Wall Cylindrical Tank. NASA TN D-3636, 1966.

8. Bukharinov, G. N.: Oscillation of Two Bodies Connected by Circular Cylindrical Shell. Investigation of Elasticity and Plasticity. Rep. FTD-MT-64-450, Air Force Systems Command, Jan. 11, 1966, pp. 93-100. (Available from DDC as AD-630414.)

9. Kana, Daniel D.; and Chu, Wen-Hwa: Influence of a Rigid Top Mass on the Response of a Pressurized Cylinder Containing Liquid. J. Spacecraft Rockets, vol. 6, no. 2, Feb. 1969, pp. 103-110.

10. Saleme, E.; and Liber, T.: Vibrations of Partially Filled Tanks. Ill. Inst. Tech. Research Inst., Oct. 1963.

11. Donnell, L. H.: Stability of Thin-Walled Tubes Under Torsion. NACA TR-479, 1933.

12. Gibson, J. E.: Linear Elastic Theory of Thin Shells. Pergamon Press, 1965, p. 36.

13. Runyan, Harry L.; Pratt, Kermit G.; and Piece, Harold B.: Some Hydro-Elastic-Pneumatic Problems Arising in the Structural Dynamics of Launch Vehicles. Paper 65-AV-27, ASME, Mar. 1965.

14. Morse, Philip M.: Vibration and Sound. Second ed., McGraw-Hill Book Co., Inc., 1948.

NATIONAL AERONAUTICS AND SPACE ADMINISTRATION
WASHINGTON, D.C. 20546

OFFICIAL BUSINESS

FIRST CLASS MAIL

POSTAGE AND FEES PAI
NATIONAL AERONAUTICS
SPACE ADMINISTRATION

POSTMASTER: If Undeliverable (Section 1
Postal Manual) Do Not Re

"The aeronautical and space activities of the United States shall be conducted so as to contribute . . . to the expansion of human knowledge of phenomena in the atmosphere and space. The Administration shall provide for the widest practicable and appropriate dissemination of information concerning its activities and the results thereof."

—NATIONAL AERONAUTICS AND SPACE ACT OF 1958

NASA SCIENTIFIC AND TECHNICAL PUBLICATIONS

TECHNICAL REPORTS: Scientific and technical information considered important, complete, and a lasting contribution to existing knowledge.

TECHNICAL NOTES: Information less broad in scope but nevertheless of importance as a contribution to existing knowledge.

TECHNICAL MEMORANDUMS: Information receiving limited distribution because of preliminary data, security classification, or other reasons.

CONTRACTOR REPORTS: Scientific and technical information generated under a NASA contract or grant and considered an important contribution to existing knowledge.

TECHNICAL TRANSLATIONS: Information published in a foreign language considered to merit NASA distribution in English.

SPECIAL PUBLICATIONS: Information derived from or of value to NASA activities. Publications include conference proceedings, monographs, data compilations, handbooks, sourcebooks, and special bibliographies.

TECHNOLOGY UTILIZATION PUBLICATIONS: Information on technology used by NASA that may be of particular interest in commercial and other non-aerospace applications. Publications include Tech Briefs, Technology Utilization Reports and Notes, and Technology Surveys.

Details on the availability of these publications may be obtained from:

SCIENTIFIC AND TECHNICAL INFORMATION DIVISION

NATIONAL AERONAUTICS AND SPACE ADMINISTRATION

Washington, D.C. 20546